

## Report CNR Short Term Mobility 2016

**Proponente:** Silvia Nappini

**Istituto di afferenza:** Istituto Officina dei Materiali CNR-IOM (Trieste)

**Qualifica:** Ricercatore livello III

### ***Electronic structure of magnetic CoFe<sub>2</sub>O<sub>4</sub> nanoparticles in liquid environment***

During the short term mobility stay (from March 28 to April 18, 2017) at the **Lawrence Berkeley National Lab (LBNL)** in Berkeley (USA) I worked in collaboration with the **beamline 6.3.1.2** staff scientists (**prof. Jinghua Guo and dr. Yi Sheng Liu**) at the **Advanced Light Source (ALS)**.

Beamline 6.3.1.2 is dedicated to *in-situ/operando* soft x-ray spectroscopy studies of samples in liquid environment.

Soft X-ray absorption spectroscopy (XAS) provides unique information, including elemental and symmetry selectivities, about the electronic structure of the chemically active atomic orbitals in materials. The effects of external factors such as temperature, pressure, electrical stimuli, light stimuli, ionic environment, pH value or different solvents can have short- and long-term kinetic influence on the electronic structure of the studied material. In order to study the electronic properties of materials in working and in environmental conditions, such as in the presence of a liquid medium or gas, special ultra-high vacuum (UHV) compatible static and/or flow cells equipped with a soft X-ray transparent thin silicon nitride (Si<sub>3</sub>N<sub>4</sub>) window are required.

The original goal of the proposal was the investigation of the electronic properties of DNA oligonucleotides immersed in their physiological environment by means of XAS measurements. Nevertheless, the setup for soft x-ray spectroscopy of liquids requires a high concentration of the elements suspended in solution to make possible their detection by XAS measurements. Unfortunately, the setup available at ALS (beamline 6.3.1.2) does not allow the detection of low concentrated DNA aqueous solution.

For this reason, we have decided to investigate the electronic properties of other promising scientific samples having suitable concentration for their characterization in liquid environment: magnetic nanoparticles. Two differently stabilized CoFe<sub>2</sub>O<sub>4</sub> nanoparticles (NPs) in aqueous solution were studied by XAS (measured in total fluorescence yield mode, TFY) at the O K-, Co L<sub>32</sub>-, Fe L<sub>32</sub>- edges: citrate coated and uncoated negatively charged NPs.

The spectroscopic investigation of magnetic CoFe<sub>2</sub>O<sub>4</sub> NPs in their liquid environment is fundamental for understanding the possible perturbations of the electronic and magnetic properties induced by the solvent in view of biomedical applications.

Magnetic nanoparticles (MNPs) have grown a great interest because of their remarkable magnetic, electric, physical and chemical properties, which, in most cases, are different from those of the bulk materials. Thanks to their intriguing properties, MNPs have found applicability in many different areas, such as fabrication of electronic components for the information storage, magnetic cards, recording devices, catalysis, and, when properly functionalized, they represent a promising approach for drug delivery, magnetic fluid hyperthermia, magnetic resonance imaging, tissue engineering and bioanalysis<sup>1-5</sup>.

The surface morphology could be modified by the presence of a coating shell which is fundamental for biomedical applications. The surface coating can regulate the physical and chemical stability of the system, preventing NPs aggregation in physiological environment, and providing also a higher biocompatibility. The NPs coating is generally obtained by chemical functionalization with organic or inorganic ligands, polymers, surfactants, dextran and phospholipids <sup>2</sup>. The nature of the surface shell can affect the water accessibility to the magnetic core, influencing also the magnetic properties and relaxivity of the MNPs.

## Experimental method

The experimental setup for the electronic characterization of samples *in-operando* at the ISAAC end station of beamline 6.3.1.2 at the Advanced Light Source (ALS) allows to operate with both static cell or flow cell mounted in a UHV chamber<sup>6,7</sup>. The beamline provides soft x rays in the energy range from 200 to 2000 eV. The energy resolution is adjustable and it was set at 0.6 eV by using 600 l/mm grating by selecting an exit slit size of 40 micro meter. During the XAS measurement, the storage ring current was 500 mA which provides a photon flux of about  $10^{11}$  photons at 530 eV.

The cell is made up with the following components: 1 mm × 1 mm Si<sub>3</sub>N<sub>4</sub> window of 100 nm thicknesses etched on a silicon frame of 10 mm × 10 mm area, and 0.5 mm thickness; a sample holder made of polyether-ether ketone (PEEK), an UHV compatible and chemically inert material, with good mechanical property and electrical insulation. The front side of the PEEK cell has a Viton O-ring and equipped with electrical feed through and feeding tubes<sup>6,7</sup>. The electrical contacts are used for electrochemistry experiments, where a copper wire is used to make electric contact to the working electrode in contact with the Si<sub>3</sub>N<sub>4</sub> surface. The counter and reference electrodes are made of platinum wire and they are in contact with the electrolyte solution inside the cell reservoir (see Figure 1).

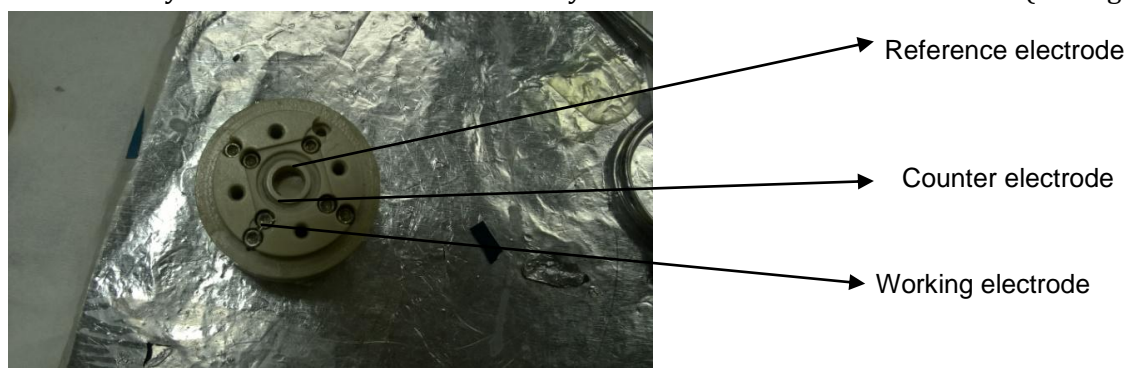


**Figure 1.** Image of the body cell reservoir with electrochemical and feeding ports.

Preliminary measurements are usually done by using a static liquid cell. A volume of about 100 µl of liquid is placed on the central holder of the body cell and covered with a Si<sub>3</sub>N<sub>4</sub> membrane. The top cap of the cell is pressed against the holder by affixing it with four metal screws as shown in Figure 2. The screws are tightened slowly so that it does not translate high stress to the membrane window. The micro-fluidic cell is used to prevent beam damage of the sample, thus fresh liquid is continuously flowed through the cell.



**Figure 2.** Image of the static liquid cell.

The microfluidic setup consists of a PEEK holder similar to the static cell. For the electrolyte supplying inside the cell, two Teflon tubes are used as inlet and outlet. The end of the Teflon tubing is separated from the cell with an interlock valve which prevents the accidental flow of liquid into experimental chamber in an unexpected event of  $\text{Si}_3\text{N}_4$  window breakage. The interlock valves are controlled by a 12 V DC valve controller. Electrolyte is carried out by a peristaltic pump operated by a PCI card operated valve controller. The feeding volume is 5 ml and the pulse rate can be tuned from 1 to 10 Hz, enabling a liquid flow rate which can be tuned in a range of 50–200  $\mu\text{l/s}$  for the replacement of liquid at a selected time interval<sup>6</sup>.

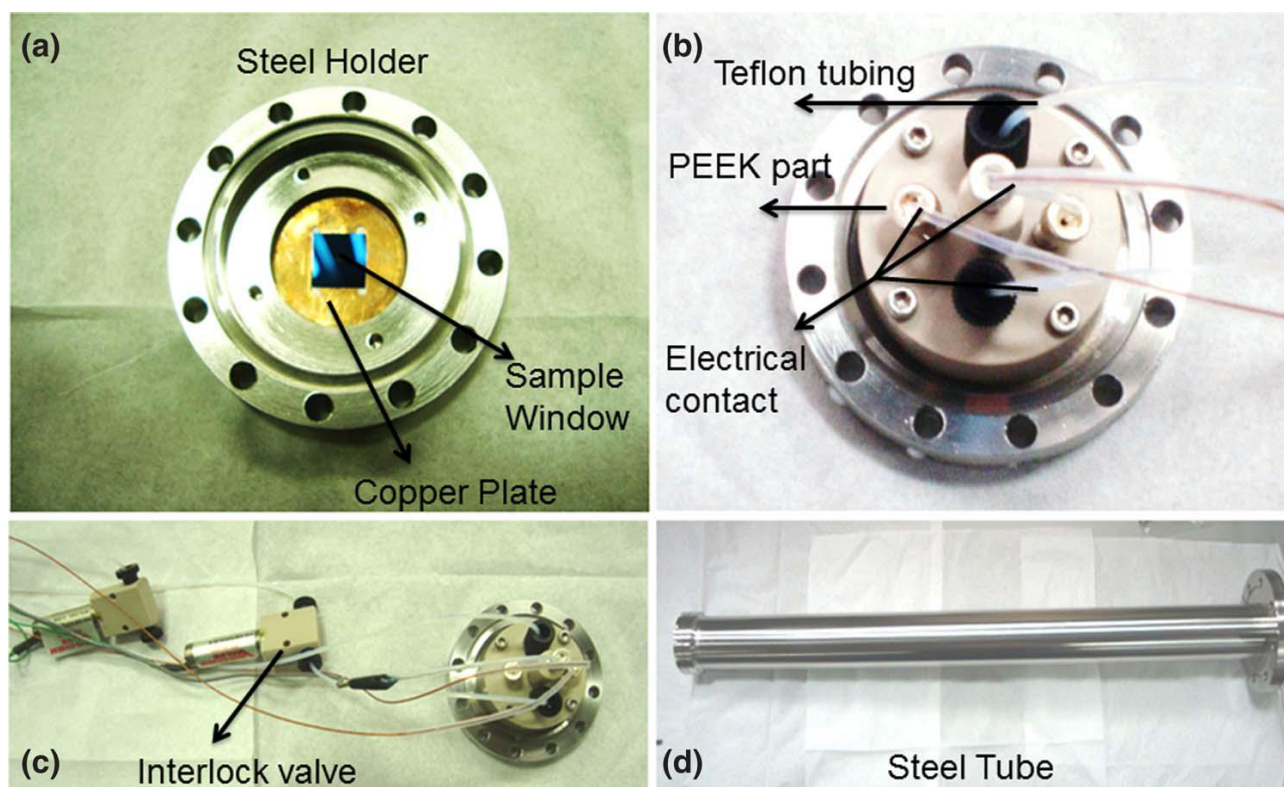


**Figure 3.** (a) The sample window sits on top of a copper plate supported by a steel holder. (b) The PEEK cell is pressed against the steel holder. (c) Overview of the whole assembly. (d) Steel tube for the UHV experiment. Figure extracted from "An ultra-high vacuum electrochemical flow cell for in situ/operando soft X-ray spectroscopy study Experiment". D. K. Bora, P.A Glans, J. Pepper, Y-S. Liu, C. Du, D. Wang, and J.-H. Guo. *Review of Scientific Instruments* 85, 043106, 2014<sup>6</sup>.

### Discussion and Results

Two different samples of  $\text{CoFe}_2\text{O}_4$  NPs suspended in aqueous solution were studied:

- 1) Uncoated NPs bearing negative surface charges,
- 2) Citrate coated  $\text{CoFe}_2\text{O}_4$  NPs

Both samples were prepared according to the method developed by Massart<sup>8</sup>. The diameter of the NPs ranges mainly from 10 to 15 nm, and are well dispersible in aqueous solution.

A schematic representation of the MNP samples is reproduced in the scheme of Figure 4.

We have recently characterized the electronic and magnetic properties of these MNPs samples deposited on Si wafers by several techniques (XPS, XAS, XMCD) at BACH beamline, Elettra synchrotron facility in Trieste<sup>8</sup>. The results on the dried film have shown that Fe is present dominantly in the +3 state, while Co is in the +2 state for all the samples. In particular  $\text{Fe}^{2+}$  ions are located at the  $\text{O}_h$  sites, while

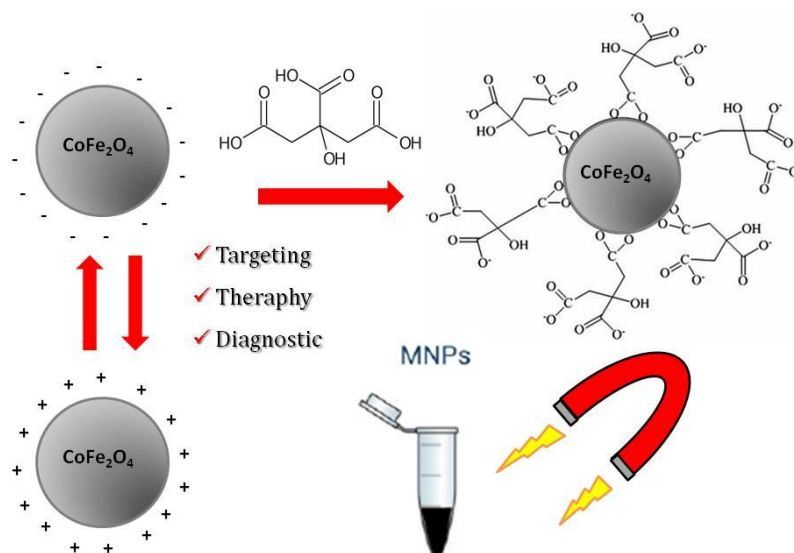


**Figure 4.** Scheme of differently stabilized  $\text{CoFe}_2\text{O}_4$  nanoparticles. Figure extracted from "*Surface Charge and Coating of  $\text{CoFe}_2\text{O}_4$  Nanoparticles: Evidence of Preserved Magnetic and Electronic Properties*". S. Nappini et al. *J. Phys. Chem. C* **2015**, 119 (45), 25529–25541<sup>8</sup>

$\text{Fe}^{3+}$  and  $\text{Co}^{2+}$  cations occupy both the  $\text{O}_h$  and  $\text{T}_d$  sites. XMCD results have evidenced that both uncoated and citrate-coated  $\text{CoFe}_2\text{O}_4$  NPs have a similar magnetic behavior, confirming that the citrate layer does not affect surface anisotropy of the particles. However, the dispersion of MNPs in a liquid medium could strongly affect their electronic and magnetic properties. For this reason the spectroscopic investigation in their liquid environment is fundamental for the understanding of possible perturbations of the electronic and magnetic properties of coated and uncoated MNPs induced by the solvent or by the stabilizing agent (i.e negative  $\text{OH}^-$  charges or citrate shell).

The electronic properties of the MNPs were studied in liquid environment by x-ray absorption measurements (XAS) in total fluorescence yield (TFY) at the Co  $\text{L}_{32^-}$ , Fe  $\text{L}_{32^-}$  and OK- edges. These techniques are element selective and involve core atomic levels probing the local electronic structure of selected species in a system and it was already demonstrated that the interaction between nanocrystals and surfactant and solvent molecules can be successfully measured by these techniques operating *in situ*<sup>9</sup>.

A volume of 100  $\mu\text{l}$  of  $\text{CoFe}_2\text{O}_4$  of both samples (30 mg/ml) were placed in the hollow of the cell and covered with a  $\text{Si}_3\text{N}_4$  100 nm window fixed by a cap. The screws were tightened in a careful manner so that it is vacuum sealed. The sealing can be visualized by the bulging of the sample window in upward direction. Before placing the cell into the experimental chamber, it was pumped down to the required pressure of at least  $2 \times 10^{-6}$  Torr in the load lock chamber so that the experimental chamber pressure holds a pressure below  $1 \times 10^{-8}$  Torr at which the channeltron is able to operate at a reduced noise

level. The translation and the position of the cell window were optimized by moving the manipulator in XYZ axis and rotating it of a suitable angle to have the cell perpendicular to the X-ray beam. The position of the beam was found by using a YAG crystal mounted on the manipulator and the energy calibration was done by measuring XAS spectra in TEY and TFY at O -K, Fe -L<sub>23</sub> and Co -L<sub>23</sub> edges of three references samples: TiO<sub>2</sub>, Fe<sub>2</sub>O<sub>3</sub> and Co<sub>3</sub>O<sub>4</sub> crystals, respectively (see Figure 5).

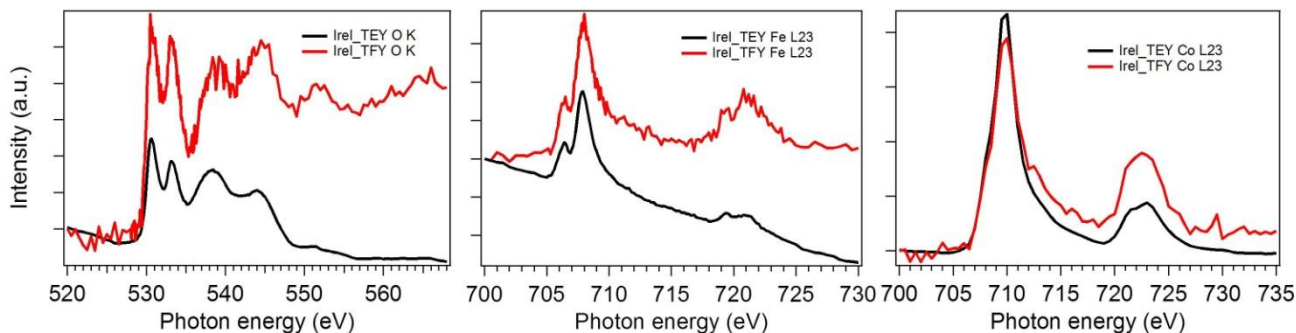


**Figure 5.** XAS of the reference spectra mounted on the manipulator. From left to right: O -K, Fe -L<sub>23</sub> and Co -L<sub>23</sub> edges, measured in TEY (black curve) and TFY (red curve).

The position of the beam was then optimized by moving XYZ around the Si<sub>3</sub>N<sub>4</sub> window area to find the liquid where the Oxygen signal from water is higher in comparison to the oxygen of the Si<sub>3</sub>N<sub>4</sub> film (see Figure 6). The signal due to H<sub>2</sub>O is located at 535 eV<sup>10</sup>, while the oxide signal from the CoFe<sub>2</sub>O<sub>4</sub> nanoparticles is located at 530 eV<sup>8</sup>.

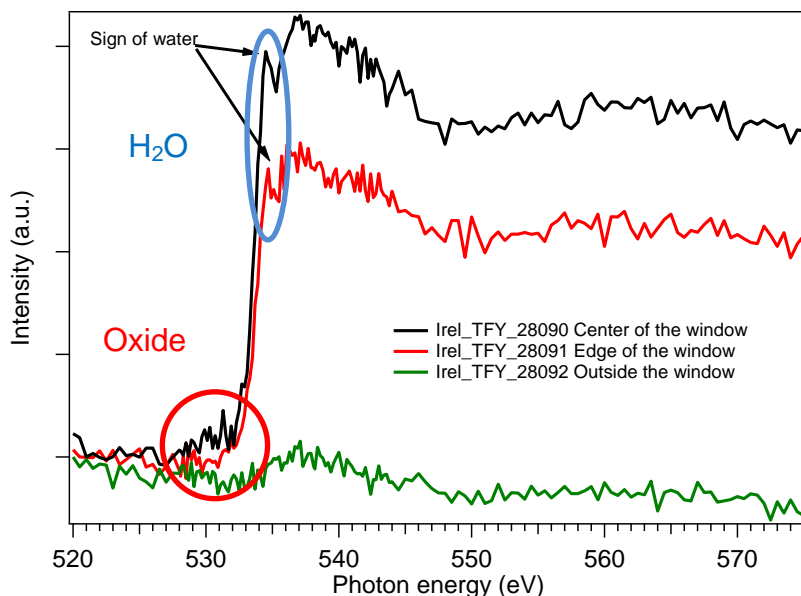


**Figure 6.** XAS spectra of O K-edge measured on the center of the window (black curve, water is visible), on the edge of the window (red curve, water is still visible) and outside the window (green curve, water is not visible anymore).

The beam was placed where the signal of water was higher (center of the window) and on this position the O-K edge, Fe L<sub>23</sub> and Co L<sub>23</sub> edges of the two CoFe<sub>2</sub>O<sub>4</sub> NPs dispersions were measured in TFY.



As shown in Figure 7, the signal arising from uncoated  $\text{CoFe}_2\text{O}_4$  is very weak, almost invisible. The low intensity at the Fe  $L_{23}$  is probably due to the precipitation of the nanoparticles on the bottom of the cell, making their analysis impossible with such low beamline flux.

In the case of citrate coated nanoparticles, no precipitation was observed on the bottom of the cell, evidencing that the citrate coating prevents aggregation phenomena and makes the nanoparticles more stable and well dispersible in aqueous environment with respect to the uncoated ones.

Fe  $L_{23}$  spectra of citrate coated NPs is reported in Figure 7, but the signal results very noisy and weak also in this case because of the low beamline flux.

Co  $L_{23}$  was also measured, but no signal was detected because its concentration is half of Fe and the cross section is even lower.

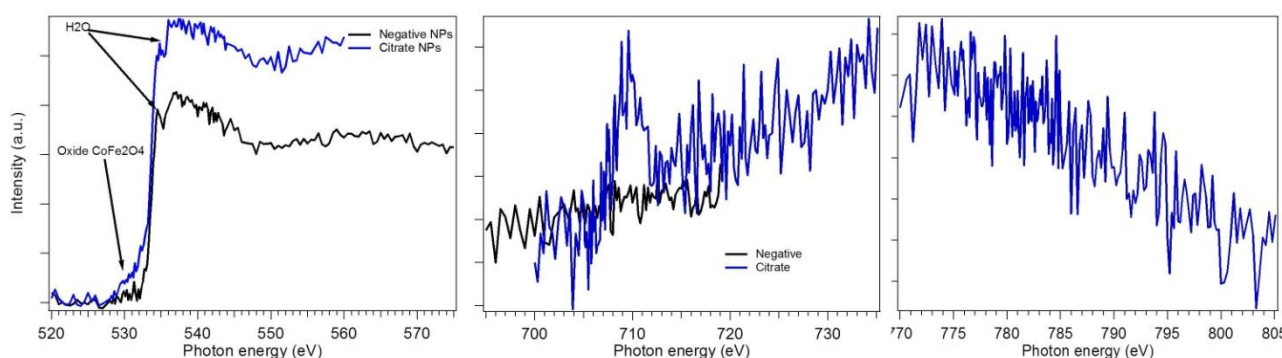


**Figure 7.** XAS spectra of citrate coated (blue spectrum) and uncoated (black spectrum)  $\text{CoFe}_2\text{O}_4$  NPs.

From left to right: O -K, Fe  $L_{23}$  and Co  $L_{23}$  edge spectra of both samples.

Because of the low signal measured in the static cell, we have decided to try the flow system to avoid unwanted precipitation of the MNPs on the bottom of the cell.

A volume of 10 mL of MNPs suspension of both samples was flowed through two teflon tubes (inlet and outlet of the cell) with a flow rate of  $50\mu\text{l}/\text{sec}$ .

The cell apparatus is similar to that of the static cell, but a channel connected to the inlet and outlet is present. A picture of the setup inside the UHV chamber is shown in Figure 8.



A picture of the setup inside the UHV chamber is shown in Figure 8.

XAS spectra at the O -K, Fe and Co - $L_{23}$  edges measured with the flow cell are reported in Figure 9. A big improvement in the signal intensity was achieved with uncoated negatively charged MNPs thanks to the continuous supply of fresh solution which allows a drastically reduction of the precipitation of the NPs.

No improvement was observed in the case of citrate coated MNPs. The low signal of the citrate coated MNPs could be due to the concentration of  $\text{CoFe}_2\text{O}_4$  which could be slightly lower than that of negatively charged MNPs.

**Figure 8.** Micro-fluidic cell in the UHV experimental chamber

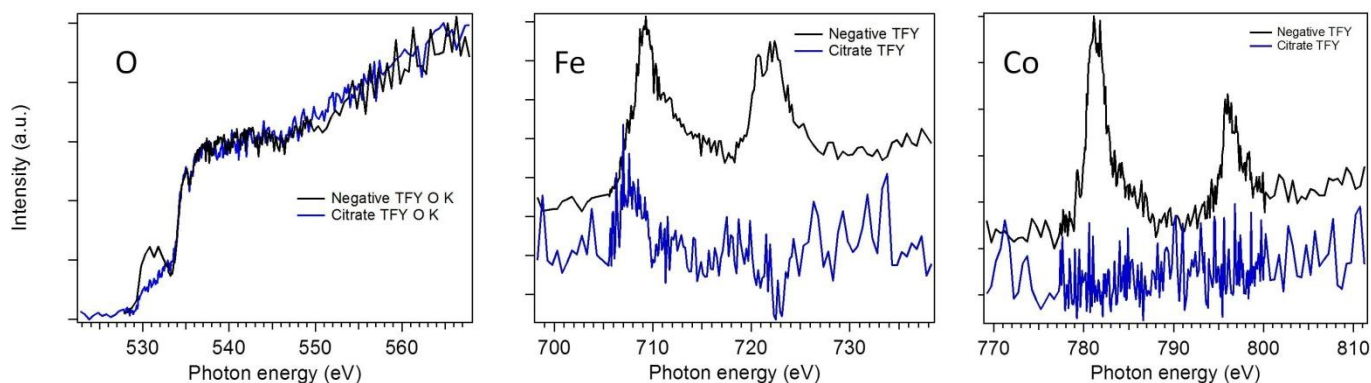


**Figure 9.** XAS spectra at the O -K, Fe and Co -L23 edges measured with the flow cell

Uncoated  $\text{CoFe}_2\text{O}_4$  NPS spectra at Fe and Co -L<sub>23</sub> edges are affected by self-absorption effects typical of TFY mode detection for high element quantities. Interestingly, a comparison with the XAS spectra of dry film of the same samples (measured at BACH beamline, Elettra Trieste) shows a different spin-orbital splitting. This effect is more evident in Fe XAS spectra and it can be related to the presence of water, which strongly interacts with Fe atoms in  $\text{CoFe}_2\text{O}_4$  NPs (see Figure 9). This interesting effect should be further investigated and understood. For these reasons additional measurements and theoretical calculation are necessary. The plan for the future is to develop a microfluidic setup for liquid based on  $\text{Si}_3\text{N}_4$  cells on the CNR beamline ,BACH, at Elettra synchrotron facility in Trieste, where we envisage repeating the same measurements with an increased signal to noise ratio.

## Conclusions

An electronic characterization of  $\text{CoFe}_2\text{O}_4$  NPs suspended in aqueous solution was performed on beamline 6.3.1.2 at ALS at the LBNL in Berkeley (CA). Two different stabilized NPs were studied: uncoated and citrate coated  $\text{CoFe}_2\text{O}_4$  NPs. Both samples have evidenced the presence of water, which is the solvent employed to suspend nanoparticles. Nevertheless, the uncoated NPs sample was affected by precipitation due to aggregation phenomena which have hindered the possibility to measure a signal from Fe and Co L-edges. The citrate coated NPs were more stable in solution, evidencing that the citrate shell is able to protect the  $\text{CoFe}_2\text{O}_4$  magnetic cores from electromagnetic aggregation. For this reason a weak signal of Fe was detected in the case of citrate coated  $\text{CoFe}_2\text{O}_4$ . The use of the flow cell allowed the measure of XAS spectra of uncoated MNPs preventing their precipitation on the bottom of the cell, and revealing a higher concentration of uncoated MNPs with respect to citrate coated MNPs. An interesting spin-orbital splitting was observed in XAS spectra at Fe and Co L<sub>23</sub> edge in liquid medium which deserves further investigations.

Unfortunately, the concentration of NPs in solution (30 mg/ml) was too low to measure high -quality spectra at beamline 6.3.1.2, which is a bend magnet beamline, and therefore it suffers of low beam flux. Thanks to STM program I believe to have gained the knowledge and the capabilities to reproduce a similar setup based on  $\text{Si}_3\text{N}_4$  cells for liquids on BACH beamline at Elettra synchrotron facility Trieste. The experiments will be repeated on high concentration  $\text{CoFe}_2\text{O}_4$  NPs.

## Reference

- (1) McBain, S. C.; Yiu, H. H.; Dobson, J. Magnetic Nanoparticles for Gene and Drug Delivery. *Int. J. Nanomedicine* **2008**, 3 (2), 169–180.
- (2) Venturelli, L.; Nappini, S.; Bulfoni, M.; Gianfranceschi, G.; Dal Zilio, S.; Coceano, G.; Del Ben, F.; Turetta, M.; Scoles, G.; Vaccari, L.; Cesselli, D.; Cojoc, D. Glucose Is a Key Driver for GLUT1-Mediated Nanoparticles Internalization in Breast Cancer Cells. *Sci. Rep.* **2016**, 6, 21629.

- (3) Bañobre-López, M.; Teijeiro, A.; Rivas, J. Magnetic Nanoparticle-Based Hyperthermia for Cancer Treatment. *Rep. Pract. Oncol. Radiother.* **2013**, *18* (6), 397–400.
- (4) Bonini, M.; Berti, D.; Baglioni, P. Nanostructures for Magnetically Triggered Release of Drugs and Biomolecules. *Curr. Opin. Colloid Interface Sci.* **2013**, *18* (5), 459–467.
- (5) Estelrich, J.; Sánchez-Martín, M. J.; Busquets, M. A. Nanoparticles in Magnetic Resonance Imaging: From Simple to Dual Contrast Agents. *Int. J. Nanomedicine* **2015**, *10*, 1727–1741.
- (6) Bora, D. K.; Glans, P.-A.; Pepper, J.; Liu, Y.-S.; Du, C.; Wang, D.; Guo, J.-H. An Ultra-High Vacuum Electrochemical Flow Cell for in Situ/operando Soft X-Ray Spectroscopy Study. *Rev. Sci. Instrum.* **2014**, *85* (4), 43106.
- (7) Guo, J.; Tong, T.; Svec, L.; Go, J.; Dong, C.; Chiou, J.-W. Soft-X-Ray Spectroscopy Experiment of Liquids. *J. Vac. Sci. Technol. A* **2007**, *25* (4), 1231–1233.
- (8) Nappini, S.; Magnano, E.; Bondino, F.; Píš, I.; Barla, A.; Fantechi, E.; Pineider, F.; Sangregorio, C.; Vaccari, L.; Venturelli, L.; Baglioni, P. Surface Charge and Coating of CoFe<sub>2</sub>O<sub>4</sub> Nanoparticles: Evidence of Preserved Magnetic and Electronic Properties. *J. Phys. Chem. C* **2015**, *119* (45), 25529–25541.
- (9) Liu, H.; Guo, Y.; Yin, Y.; Augustsson, A.; Dong, C.; Nordgren, J.; Chang, C.; Alivisatos, P.; Thornton, G.; Ogletree, D. F.; Requejo, F. G.; de Groot, F.; Salmeron, M. Electronic Structure of Cobalt Nanocrystals Suspended in Liquid. *Nano Lett.* **2007**, *7* (7), 1919–1922.
- (10) Velasco-Velez, J.-J.; Wu, C. H.; Pascal, T. A.; Wan, L. F.; Guo, J.; Prendergast, D.; Salmeron, M. The Structure of Interfacial Water on Gold Electrodes Studied by X-Ray Absorption Spectroscopy. *Science* **2014**, *346* (6211), 831–834.